Ukrainian Journal of Physical Optics
SPECIAL ISSUE 5, 2024

Bright and Dark Solitons in a (2+1)-Dimensional Spin-1 Bose-Einstein Condensates

Nan Li[1], Quan Chen[1], Houria Triki[2], Feiyan Liu[3], Yunzhou Sun[1,3], Siliu Xu[4], Qin Zhou[3]

[1]Hubei Province Engineering Research Center for Intelligent Micro-Nano Medical Equipment and Key Technologies, School of Electronic and Electrical Engineering, Wuhan Textile University, Wuhan 430200, China, chenquan1977@126.com
[2]Radiation Physics Laboratory, Department of Physics, Faculty of Sciences, Badji Mokhtar University, P.O. Box 12, 23000 Annaba, Algeria
[3]Research Center of Nonlinear Science, School of Mathematical and Physical Sciences, Wuhan Textile University, Wuhan 430200, China, syz@wtu.edu.cn
[4]School of Biomedical Engineering and Medical Imaging, Xianning Medical College, Hubei University of Science and Technology, Xianning 437100, China

Received: 29.12.2023

Abstract. The three-coupled Gross-Pitaevskii equation with a harmonic potential in a (2+1)-dimensional spin-1 Bose-Einstein condensate is studied in this paper. Using the Hirota bilinear method, the bright and dark soliton solutions of the system with attractive and repulsive interactions are obtained, and the amplitudes and velocities of those solitons are also given. In addition, we analyze the influence of harmonic potential on the dynamics of solitons and discuss the interaction between solitons through asymptotic analysis. As a result, we find that the amplitude and velocity of solitons are related to the harmonic potential, and the interaction between the two solitons is elastic.

Keywords: soliton, Hirota bilinear method, asymptotic analysis, Bose-Einstein condensates
UDC: 535.32
DOI: 10.3116/16091833/Ukr.J.Phys.Opt.2024.S1060

1. Introduction

In recent years, as a localized wave that can propagate undistorted in nonlinear physical media, the study of solitons has attracted increasing attention [1–3]. The main mechanism to generate these self-maintaining localized waves is the balance between the dispersion and nonlinearity effects. A particularly interesting property of solitons is their robust nature, displayed in their propagation dynamics and interaction process. This fascinating property makes them physically relevant nonlinear waves that are potentially useful in various practical applications. Experimentally, solitons are widely observed in various nonlinear physical systems, such as nonlinear optics, fluid dynamics, Bose-Einstein condensates (BECs), and so on [4, 5]. Regarding optical contexts, two distinct kinds of solitons, called bright and dark solitons, can be formed in the nonlinear media with anomalous and normal dispersion regimes, respectively. Taking advantage of several differences between such soliton types, a rich variety of powerful applications have been demonstrated with their utilization, including all-optical proceeding, signal transmission, switching, and many other optical applications related to condensed matter systems.

The diluted gas BECs provide an ideal experimental platform for studying matter-wave solitons. At sufficiently low temperatures, the range of the atomic fluctuation behavior exceeds the average distance between two atoms, and all atoms coalesce into a single quantum state with the lowest energy. This phenomenon is called BEC [6]. The particles in BEC have the same quantum state and the same dynamical properties. BEC promotes the development of related disciplines and has been widely used in fields such as cold atomic clocks, cold atomic interferometers, and optical tweezers [7–9]. In addition, matter-wave solitons in BEC allow the development of a new generation of electronic circuits and quantum computers [10]. At present, the nonlinear phenomena of BEC, such as solitons, superfluidity, and vortices, are still hot issues in research [11,12].

Simply considering two contact interactions between atoms, the evolution of the condensate can be described by the Gross-Pitaevskii (GP) equation, which provides a reliable guide to the analytic study of solitons in this system [13]. This accurate mean-field model generally incorporates an external potential accounting for the magnetic, optical, or combined confinement of dilute alkali vapors that constitute the BEC. Typically, the GP equation for a single-component BEC is integrable and confined in a one-dimensional magnetic traps potential system and generates matter-wave bright/dark solitons in experiments [14–17]; such bright/dark solitons in BECs have also been studied extensively theoretically [18–22]. Moreover, in the higher-dimensional BEC model, in a large amount of theoretical work, the soliton solutions have been obtained and their interactions have been analyzed [23–28].

In an optical trap potential, due to interparticle interactions of atoms, the direction of atomic spins changes [29]. Accordingly, the order parameter of a spin-F BEC is described by a macroscopic wave function with $2F$+1 components, which can vary over space and time. Currently, a part of the theoretical work has solved for multi-component vector solitons in spin BEC [30], correlated studies have shown a variety of interesting phenomena in this context [31, 32], including bright solitons [33], dark solitons [34], gap solitons [35], complex vector solitons [36], rogue wave [37], the nonautonomous ferromagnetic and polar solitons [38, 39]. So far, many analytical methods, such as bilinear methods, Darboux transformation methods, self-similarity transformation methods, and some numerical methods, have been used to solve nonlinear equations [40–42]. Among all the known methods, the Hirota bilinear technique is one of the most efficient methods to derive multi-soliton solutions of the GP equation (and its variants). It has been utilized in a number of works. It is worth mentioning that the research on multi-component GP equations mainly focuses on one dimension, and most of them are solved and analyzed using numerical methods. We should point out that the multidimensional nature of nonlinear dispersive waves may offer a number of novel features that are not found in the one-dimensional case, for example, by discovering novel multi-humped solitonic structures. Moreover, solutions in analytic form, when they exist for multidimensional nonlinear wave equations, can help one understand the dynamical processes and physical phenomena governed by these equations. To our knowledge, there have been no reported bright and dark soliton solutions obtained through resolution for the three-component GP equation. This work will consider two-dimensional GP equations with F=1 at a harmonic potential. In a two-dimensional harmonic potential, spin-1 GP equations with a harmonic potential can be written as [43, 44]

$$
\begin{aligned}
&i\phi_{\pm1,t}+\phi_{\pm1,xx}+\phi_{\pm1,yy}+2\sigma\left(\left|\phi_{\pm1}\right|^2+2\left|\phi_0\right|^2\right)\phi_{\pm1}+2\sigma\phi_0^2\phi_{\mp1}^*+u_{ext}(x,y)\phi_{\pm1}=0,\\
&i\phi_{0,t}+\phi_{0,xx}+\phi_{0,yy}+2\sigma\left(\left|\phi_{+1}\right|^2+\left|\phi_{-1}\right|^2+\left|\phi_0\right|^2\right)\phi_0+2\sigma\phi_0^*\phi_{+1}\phi_{-1}+u_{ext}(x,y)\phi_0=0,
\end{aligned}
\tag{1}
$$

where the distribution of atoms BEC is presented by the three-component macroscopic BEC wave function $\phi(r,t)=[\phi_{-1}(r,t),\phi_0(r,t),\phi_{+1}(r,t)]^T$, the superscript T represents transpose, with the components corresponding to the three values of the vertical spin projection $m_F=-1,0,+1$, and m_F is the magnetic quantum number. Also, u_{ext} denotes the harmonic potential defined by $u_{ext}(x,y)=\Omega^2(x^2+y^2)/2$, with $\Omega=\omega_r/\omega_z$, ω_r and ω_z being the confinement frequencies in the radial and axial directions. With the assumption that $\omega_r >> \omega_z$, the motion of atoms in the Z direction is essentially frozen in the ground state of the axial harmonic trapping potential, therefore, the three-dimensional GP equation can be transformed to the aforementioned quasi two-dimensional form [45]. Additionally, when $\sigma=1$, the interactions between atoms in Eq. (1) are attractive, so one can obtain bright solitons. Conversely, when $\sigma=-1$, the inter-atomic interactions in Eq. (1) are repulsive, the dark solitons can be obtained. We note in passing that the three-component soliton complexes of the dark-dark-bright and dark-bright-bright kinds have been experimentally generated in an $F=1$ condensate of 87Rb atoms [43].

In this letter, for the first time to our knowledge, we construct a bilinear form of coupled GP equations and derive the bright/dark one-soliton and two-soliton solutions by employing the Hirota bilinear method. Interestingly, no a priori constraints have been imposed on the physical parameters to find these soliton structures. Then, the analysis of soliton solutions provides the amplitude and velocity of bright/dark one-solitons. Finally, the elastic interaction between the bright/dark two-solitons will be discussed, via the asymptotic analysis.

2. Bilinear form

We first present the bilinear form that can be applied to generate the bright and the dark one- and two-soliton solutions of the above coupled GP equations in (2+1)-dimensions. To construct the Hirota bilinear form, the variable transformations are given by [46]

$$\phi_j=e^{\frac{\sqrt{2}i\Omega}{4}(x^2+y^2)-\sqrt{2}\Omega t}\,\frac{g^{(j)}(e^{-\sqrt{2}\Omega t}x,e^{-\sqrt{2}\Omega t}y,t)}{f(e^{-\sqrt{2}\Omega t}x,e^{-\sqrt{2}\Omega t}y,t)}, \tag{2}$$

where $g^{(j)}$ are complex functions, and f is a real function of x,y,t. The bilinear form of Eq. (1) can be expressed as

$$\begin{aligned}
&\left(iD_t+e^{-2\sqrt{2}\Omega t}D_x^2+e^{-2\sqrt{2}\Omega t}D_y^2-e^{-2\sqrt{2}\Omega t}\lambda\right)g^{(\pm1)}f=0,\\
&\left(iD_t+e^{-2\sqrt{2}\Omega t}D_x^2+e^{-2\sqrt{2}\Omega t}D_y^2-e^{-2\sqrt{2}\Omega t}\lambda\right)g^{(0)}f=0,\\
&\left(D_x^2+D_y^2-\lambda\right)f\times f-2\sigma(\left|g^{(+1)}\right|^2+\left|g^{(-1)}\right|^2+2\left|g^{(0)}\right|^2)=0,\\
&\left[g^{(0)}\right]^2-g^{(+1)}g^{(-1)}=0,
\end{aligned} \tag{3}$$

where λ is a real constant, D_x,D_y and D_t are bilinear derivative operators that have been defined in Ref. [47].

2.1. Bright soliton solutions

To derive the bright one-soliton solutions of Eq. (1), we set $\lambda=0$ in the bilinear form (3). The expansion formers of $g^{(j)}$ and f with respect to the small parameter ε are truncated as

$$g^{(j)}=\varepsilon g_1^{(j)},\ f=1+\varepsilon^2 f_2, \tag{4}$$

with

$$g_1^{(j)}=\beta_j e^{\eta_1},\ f_2=ne^{\eta_1+\eta_1^*},$$
$$\eta_1=\kappa_1 x+\iota_1 y+\omega_1(t)+\eta_1^0, \tag{5}$$

where the superscript $*$ denotes the complex conjugate, η_1 is complex function of x,y and t, $\omega_1(t)$ is complex function, $\beta_j,n,\kappa_1,\iota_1$ are all arbitrary complex constants, and η_1^0 is the real one. Substituting Eqs. (4) and (5) into Eq. (3), we can collect the coefficients with the same power terms of ε to zero, and then the bright one-soliton solutions with $\varepsilon=1$ can be simplified as

$$\phi_j(x,y,t)=e^{\frac{\sqrt{2}i\Omega}{4}(x^2+y^2)-\sqrt{2}\Omega\, t}\times\frac{\beta_j e^{\kappa_1 e^{-\sqrt{2}\Omega\, t}x+\iota_1 e^{-\sqrt{2}\Omega\, t}y+\omega_1(t)+\eta_1^0}}{1+ne^{\kappa_1 e^{-\sqrt{2}\Omega\, t}x+\iota_1 e^{-\sqrt{2}\Omega\, t}y+\omega_1(t)+\kappa_1^* e^{-\sqrt{2}\Omega\, t}x+\iota_1^* e^{-\sqrt{2}\Omega\, t}y+\omega_1^*(t)+2\eta_1^0}}, \tag{6}$$

with

$$\omega_1[t]=-\frac{ie^{-2\sqrt{2}\Omega\, t}\left(\iota_1^2+\kappa_1^2\right)}{2\sqrt{2}\Omega},\ \beta_{+1}=\frac{\beta_0^2}{\beta_{-1}},\ n=\frac{(|\beta_0|^2+|\beta_{-1}|^2)\sigma}{|\beta_{-1}|^2\left[\left(\iota_1+\iota_1^*\right)^2+\left(\kappa_1+\kappa_1^*\right)^2\right]}. \tag{7}$$

To secure the two-soliton solution of Eq. (1), the expansion formers are truncated as

$$g^{(j)}=\varepsilon g_1^{(j)}+\varepsilon^3 g_3^{(j)},\ f=1+\varepsilon^2 f_2+\varepsilon^4 f_4, \tag{8}$$

with

$$g_1^{(j)}=\beta_{(j)}e^{\eta_1}+\alpha_{(j)}e^{\eta_2},\ g_3^{(j)}=L_j e^{\eta_1+\eta_1^*+\eta_2}+S_j e^{\eta_1+\eta_2^*+\eta_2},$$
$$f_2=n_1 e^{\eta_1+\eta_1^*}+n_2 e^{\eta_2+\eta_2^*}+n_3 e^{\eta_1+\eta_2^*}+n_4 e^{\eta_2+\eta_1^*}, \tag{9}$$
$$f_4=n_5 e^{\eta_1+\eta_1^*+\eta_2+\eta_2^*},\ \eta_i=\kappa_i x+\iota_i y+\omega_i(t)+\eta_i^0,$$

where η_i $(i=1,2)$ are complex functions of x,y and t, $\omega_i(t)$ $(i=1,2)$ are complex functions, η_i^0 $(i=1,2)$ are real constants, and ι_i,κ_i $(i=1,2)$, β_j,α_j,L_j,S_j, $(j=\pm1,0)$, n_j $(j=1,2,3,4,5)$ are complex constants. Substituting the above expressions into Eq. (3), the bright two-soliton solutions are given by

$$\phi_j(x,y,t)=e^{\frac{\sqrt{2}i\Omega}{4}\left(x^2+y^2\right)-\sqrt{2}\Omega\, t}\times\frac{\left(\beta_j e^{\eta_1}+\alpha_j e^{\eta_2}+L_j e^{\eta_1+\eta_1^*+\eta_2}+S_j e^{\eta_1+\eta_2^*+\eta_2}\right)}{1+n_1 e^{\eta_1+\eta_1^*}+n_2 e^{\eta_2+\eta_2^*}+n_3 e^{\eta_1+\eta_2^*}+n_4 e^{\eta_2+\eta_1^*}+n_5 e^{\eta_1+\eta_1^*+\eta_2+\eta_2^*}}. \tag{10}$$

The parameters of Eq. (10) are listed in the Appendix.

2.2. Dark soliton solutions

To derive the dark one-soliton solutions for Eq. (1), we assume λ is a positive real number, with respect to the small parameter ε, the expansion formers of $g^{(j)}$ and f are truncated as

$$g^{(j)}=g_0^{(j)}(1+\varepsilon g_1^{(j)}),\ f=1+\varepsilon f_1, \tag{11}$$

with

$$g_0^{(j)}=p_j e^{i\rho(t)},\ g_1^{(j)}=e^{\xi_1+2i\theta},\ f_1=e^{\xi_1},$$
$$\xi_1=\kappa_1 x+\iota_1 y+\omega_1(t)+\xi_1^0, \tag{12}$$

where ξ_1 is real function of x, y and t, $\omega_1(t), \rho(t)$ are both real functions, $p_j\ (j=\pm1,0)$ are complex constants, $\kappa_1, \iota_1, \xi_1^0, \theta$ are the real ones, and θ ranges from 0 to 2π. Substituting Eqs. (11) and (12) into the Eq. (3), then the dark one-soliton solutions can be expressed as

$$\phi_j(x,y,t)=e^{\frac{\sqrt{2}i\Omega}{4}(x^2+y^2)-\sqrt{2}\Omega t}\frac{p_j e^{i\rho(t)}\left(1+e^{\kappa_1 e^{-\sqrt{2}\Omega t}x+\iota_1 e^{-\sqrt{2}\Omega t}y+\omega_1(t)+\xi_1^0+2i\theta}\right)}{1+e^{\kappa_1 e^{-\sqrt{2}\Omega t}x+\iota_1 e^{-\sqrt{2}\Omega t}y+\omega_1(t)+\xi_1^0}}, \tag{13}$$

with

$$\begin{aligned}&\rho(t)=\frac{e^{-2\sqrt{2}\Omega t}\lambda}{2\sqrt{2}\Omega},\ p_{-1}=\frac{p_0^2}{p_1},\ \lambda=-2\left(2|p_0|^2+|p_1|^2+|p_{-1}|^2\right)\sigma,\\ &\omega_1(t)=-(\iota_1^2+\kappa_1^2)\frac{e^{-2\sqrt{2}\Omega t}}{2\sqrt{2}\Omega}\cot\theta,\ |p_0|^2=-|p_1|^2\pm\frac{i\sqrt{|p_1|^2(\iota_1^2+\kappa_1^2)\sigma}\csc\theta}{2\sigma}.\end{aligned} \tag{14}$$

To secure the two-soliton solution of Eq. (1), the expansion formers are truncated as

$$g^{(j)}=g_0^{(j)}\left(1+\varepsilon g_1^{(j)}+\varepsilon^2 g_2^{(j)}\right),\ f=1+\varepsilon f_1+\varepsilon^2 f_2, \tag{15}$$

with

$$\begin{aligned}&g_0^{(j)}=p_j e^{i\rho(t)},\ g_1^{(j)}=e^{\xi_1+2i\theta_1}+e^{\xi_2+2i\theta_2},\ g_2^{(j)}=d_j e^{\xi_1+2i\theta_1+\xi_2+2i\theta_2},\\ &f_2=Ae^{\xi_1+\xi_2},\ f_4=e^{\xi_1}+e^{\xi_2},\ \xi_i=\kappa_i x+\iota_i y+\omega_i(t)+\xi_i^0,\end{aligned} \tag{16}$$

where $\xi_i\ (i=1,2)$ are real functions of x, y and t, $\omega_i(t)\ (i=1,2)$ are complex functions, $p_j\ (j=\pm1,0)$ are arbitrary constants, and $\iota_i, \kappa_i, \xi_i^0, \theta_i\ (i=1,2), d_j\ (j=\pm1,0), A$ are all real constants, and θ_i range from 0 to 2π. Hence, the dark two-soliton solution can be constructed as

$$\begin{aligned}\phi_j(x,y,t)=&\,e^{\frac{\sqrt{2}i\Omega}{4}(x^2+y^2)-\sqrt{2}\Omega t}\\ &\times\frac{p_j e^{i\rho(t)}\left(1+e^{\xi_1+2i\theta_1}+e^{\xi_2+2i\theta_2}+d_j e^{\xi_1+2i\theta_1+\xi_2+2i\theta_2}\right)}{1+e^{\xi_1}+e^{\xi_2}+Ae^{\xi_1+\xi_2}}.\end{aligned} \tag{17}$$

The parameters of Eq. (17) are listed in the Appendix.

3. Dynamics of the one-soliton

Here, we will analyze the soliton solutions obtained in the previous sections. The bright one-soliton solutions of Eq. (1) are obtained from Eq. (6) it can be expressed as

$$\phi_j=\frac{\beta_j e^{-\sqrt{2}\Omega t}e^{i\chi_1(x,y,t)}}{2\sqrt{n}}\operatorname{sech}\left(\gamma_1(x,y,t)+\ln\sqrt{n}\right), \tag{18}$$

where $\chi_1(x,y,t), \gamma_1(x,y,t)$ are the real functions denoted as

$$\begin{aligned}\chi_1(x,y,t)=&\,e^{-\sqrt{2}\Omega t}(\kappa_{1I}x+\iota_{1I}y)\\ &+\left(\kappa_{1I}^2-\kappa_{1R}^2+\iota_{1I}^2-\iota_{1R}^2\right)\frac{e^{-2\sqrt{2}\Omega t}}{2\sqrt{2}\Omega}+\frac{\sqrt{2}\Omega}{4}\left(x^2+y^2\right),\\ \gamma_1(x,y,t)=&\,e^{-\sqrt{2}\Omega t}(\kappa_{1R}x+\iota_{1R}y)\\ &+\left(2\kappa_{1R}\kappa_{1I}+2\iota_{1R}\iota_{1I}\right)\frac{e^{-2\sqrt{2}\Omega t}}{2\sqrt{2}\Omega}+\eta_1^0.\end{aligned} \tag{19}$$

The subscripts R and I denote the real and imaginary parts. The amplitudes of the solitons can be summarized as $\left|\frac{\beta_j e^{-\sqrt{2}\Omega t}}{2\sqrt{n}}\right|$. Thus, the amplitudes of the solitons are mainly determined by the parameters $\beta_0, \beta_{-1}, \kappa_1, \iota_1, \Omega, \sigma$. Characteristic-line employed for propagation of the bright one-soliton can be written as

$$\kappa_{1R}e^{-\sqrt{2}\Omega\, t}x + \iota_{1R}e^{-\sqrt{2}\Omega\, t}y + \left(\kappa_{1R}\kappa_{1I} + \iota_{1R}\iota_{1I}\right)\frac{e^{-2\sqrt{2}\Omega\, t}}{\sqrt{2}\Omega} + \eta_1^0 + \ln\sqrt{n} = const. \tag{20}$$

Where *const* is an arbitrary constant. Deriving the differential Eq. (20) with respect to t, the soliton velocity $\left(\upsilon_x, \upsilon_y\right)^T$ can be expressed as

$$\upsilon_x = \upsilon_y = \frac{\sqrt{2}\Omega e^{\sqrt{2}\Omega\, t}C_1(t) - 2\left(\kappa_{1R}\kappa_{1I} + \iota_{1R}\iota_{1I}\right)e^{-\sqrt{2}\Omega t}}{\kappa_{1R}}, \tag{21}$$

$C_1(t) = const - \left(\kappa_{1R}\kappa_{1I} + \iota_{1R}\iota_{1I}\right)\frac{e^{-2\sqrt{2}\Omega\, t}}{\sqrt{2}\Omega} - \eta_1^0 - \ln\sqrt{n})$ is a real function. Therefore, the soliton velocity is not only determined by the amplitude parameters but also affected by the coefficient η_1^0. Since there are similar properties between the three components ϕ_j, we will only analyze the component ϕ_{+1} as an example.

Now we will discuss the propagation properties of the bright one-soliton. Fig. 1a presents the change of the bright one-soliton with respect to the coordinates x and y for different *t*. It is clearly found that the soliton amplitude decreases significantly with the increase of t, and the soliton amplitude tends to be close to 0 when t is increased to a certain value, which is consistent with the results of Eq. (18). The soliton velocity also changes during the propagation process, and this property is consistent with the analysis of Eq. (21). Next, we will discuss the influence of various parameters on the structure of the bright one-soliton at the same t. Firstly, compared with Fig. 1a$_2$, the value of parameter κ_1 will have a significant impact on the propagation direction and amplitude of bright solitons, as shown in Fig. 1b. Fig. 1c shows that as the intensity of the harmonic potential parameter Ω increases, the amplitude of the bright soliton decreases. Secondly, from Fig. 1b and Fig. 1d, it can be seen that if the intensity of the harmonic potential parameter Ω is reduced, the position of the soliton changes, and the velocity of the soliton decreases, but the amplitude change is relatively small.

To analyze the propagation properties and interactions of the dark solitons, the intensity of the soliton based on the dark one-soliton solutions Eq. (13) is given by

$$\left|\phi_j\right|^2 = e^{-2\sqrt{2}\Omega\, t}\left|p_j\right|^2\left[1 - \sin^2(\theta)\mathrm{sech}^2(\frac{\xi_1}{2})\right], \tag{22}$$

where $\xi_1 = e^{-\sqrt{2}\Omega\, t}(\kappa_1 x + \iota_1 y) - \left(\iota_1^2 + \kappa_1^2\right)\cot(\theta)\frac{e^{-2\sqrt{2}\Omega\, t}}{2\sqrt{2}\Omega} + \xi_1^0$ is a real function. Then the amplitude of dark one-soliton solutions is written as $e^{-\sqrt{2}\Omega\, t}\left|p_j\right|(1 - \left|\cos(\theta)\right|)$. Therefore, the soliton amplitude is determined by the parameters p_j, θ and Ω. Ω is fixed to a positive number, and the soliton amplitude decreases significantly with increasing time t. To derive the propagation velocity of the soliton, characteristic-line employed for propagation of the dark one-soliton is expressed as

$$e^{-\sqrt{2}\Omega\, t}(\kappa_1 x + \iota_1 y) - \left(\iota_1^2 + \kappa_1^2\right)\cot(\theta)\frac{e^{-2\sqrt{2}\Omega\, t}}{2\sqrt{2}\Omega} + \xi_1^0 = const. \tag{23}$$

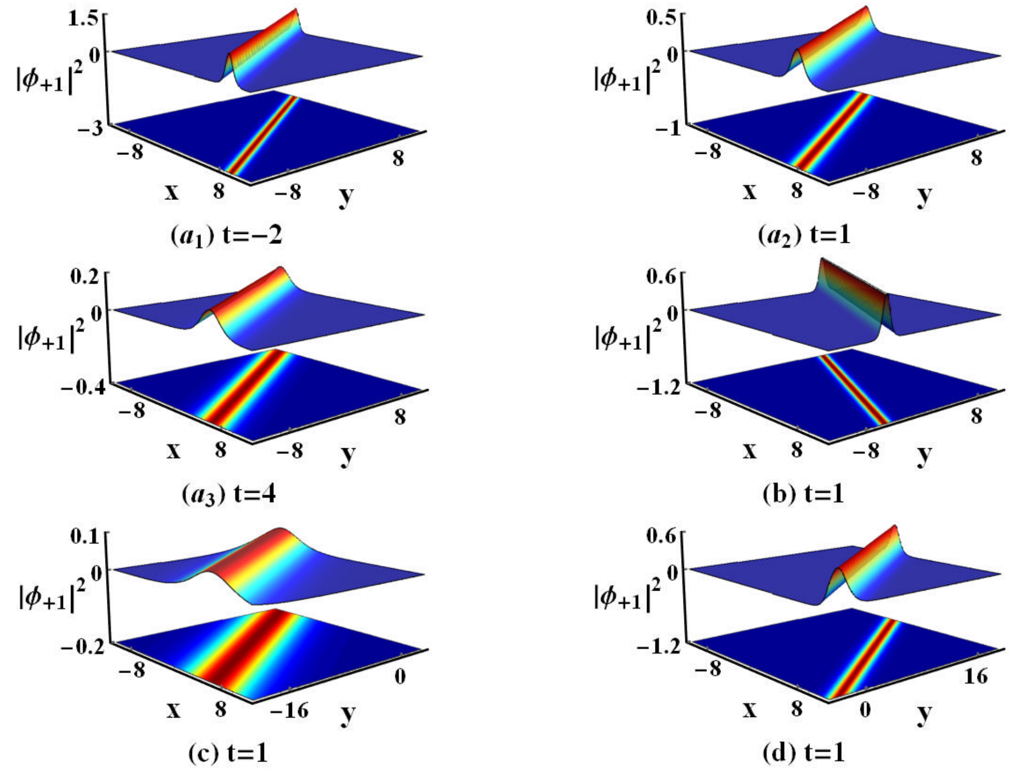

Fig. 1. The spatial-temporal evolution of the bright one-soliton solutions via Eq. (6). The parameters are $\eta_1^0 = 1$, $\beta_{-1} = \sqrt{2} + i$, $\beta_0 = 2 + \sqrt{2}i/2$, $\sigma = 1$, $\iota_1 = \sqrt{2}/2 - i$; (a) $\kappa_1 = 1 + i/2$, $\Omega = 1/8$; (b) $\kappa_1 = 1 + 1/4$, $\Omega = 1/8$; (c) $\kappa_1 = 1 + i/2$, $\Omega = 1$; (d) $\kappa_1 = 1 + i/4$, $\Omega = 1/80$.

Differentiating the distance of two characteristic lines with respect to t, the soliton velocity $\left(\upsilon_x, \upsilon_y\right)^T$ can be expressed as

$$\upsilon_x = \upsilon_y = \frac{\sqrt{2}\Omega e^{\sqrt{2}\Omega\, t} C_2(t) - e^{-\sqrt{2}\Omega\, t}\left(\iota_1^2 + \kappa_1^2\right)\cot(\theta)}{\kappa_1}, \tag{24}$$

where $C_2(t) = const + \left(\iota_1^2 + \kappa_1^2\right)\cot(\theta)\dfrac{e^{-2\sqrt{2}\Omega\, t}}{2\sqrt{2}\Omega} - \xi_1^0$ is a real function, which indicates that the velocities of the dark soliton are related to the parameters $\iota_1, \kappa_1, \Omega, \theta$.

To discuss the propagation properties of the dark soliton, the dark one-soliton solutions with respect to the coordinates x and y are shown in Fig. 2. Figs. 2a shows the dark soliton structure with time t for the same parameters. As t increases, the background plane for dark soliton propagation becomes lower, while the soliton amplitude decreases. When t increases to a certain value, the amplitude of the soliton tends to 0. This property is consistent with the analysis of Eq. (22). At $t = 1$, the effect of different parameters on the soliton structure is also analyzed. Compared to Fig. 2a$_2$, the soliton amplitude remains unchanged, and the soliton propagation direction changes by decreasing κ_1 in Fig. 2b. Increasing the strength Ω of the harmonic potential in Fig. 2c, the background plane of the dark soliton decreases while the soliton amplitude decreases. Conversely, reducing the strength of the harmonic potential Ω in Fig. 2d, the background plane of the dark soliton is raised, and the soliton amplitude increases; other properties are the same as in Fig. 2a$_2$.

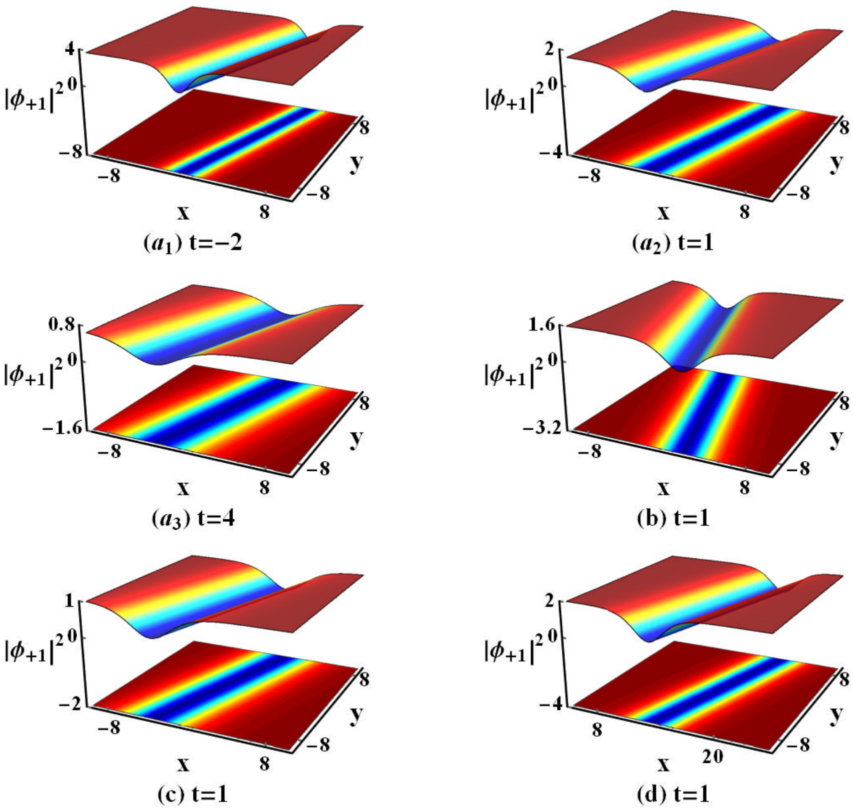

Fig. 2. The spatial-temporal evolution of the dark one-soliton via solutions (13). The parameters are $\varepsilon=1,\ \eta_1^0=1,\ \sigma=-1,\ \iota_1=-1/4,\ p_1=1+i,\ \theta=\pi/3$; (a) $\Omega=1/10,\ \kappa_1=1$; (b) $\Omega=1/10,\ \kappa_1=-1$; (c) $\Omega=1/4,\ \kappa_1=1$; (d) $\Omega=1/80,\ \kappa_1=1$.

4. Interaction analysis of the two-soliton

To discuss the interaction property between the bright two-solitons, we perform the asymptotic analysis of soliton solutions Eq. (10). In the following section, the expressions before the interaction of the two-solitons are denoted by $\phi_{+1}^{1-},\phi_{+1}^{2-}$, while the expressions after the interaction of the two-solitons are denoted by $\phi_{+1}^{1+},\phi_{+1}^{2+}$, respectively.

Through calculating the equations between η_1 and η_2, we assume $(\iota_1^2+\kappa_1^2)\kappa_2<(\iota_2^2+\kappa_2^2)\kappa_1,\ \iota_1\kappa_2<\iota_2\kappa_1$, and the asymptotic patterns are derived to be expressed as

$$\begin{aligned}
\phi_{+1}^{1-}&=\frac{S_1 e^{\sqrt{2}\Omega\, t}e^{i\chi_1(x,y,t)}}{2\sqrt{n_2 n_5}}\operatorname{sech}\left(\gamma_1(x,y,t)+\ln\sqrt{\frac{n_5}{n_2}}\right),\ (\eta_1+\eta_1^*\sim 0,\eta_2+\eta_2^*\sim+\infty),\\
\phi_{+1}^{1+}&=\frac{\beta_1 e^{\sqrt{2}\Omega\, t}e^{i\chi_1(x,y,t)}}{2\sqrt{n_1}}\operatorname{sech}\left(\gamma_1(x,y,t)+\ln\sqrt{n_1}\right),\ (\eta_1+\eta_1^*\sim 0,\eta_2+\eta_2^*\sim-\infty),\\
\phi_{+1}^{2-}&=\frac{L_1 e^{\sqrt{2}\Omega\, t}e^{i\chi_2(x,y,t)}}{2\sqrt{n_1 n_5}}\operatorname{sech}\left(\gamma_2(x,y,t)+\ln\sqrt{\frac{n_5}{n_1}}\right),\ (\eta_1+\eta_1^*\sim+\infty,\eta_2+\eta_2^*\sim 0),\\
\phi_{+1}^{2+}&=\frac{\alpha_1 e^{\sqrt{2}\Omega\, t}e^{i\chi_2(x,y,t)}}{2\sqrt{n_2}}\operatorname{sech}\left(\gamma_2(x,y,t)+\ln\sqrt{n_2}\right),\ (\eta_1+\eta_1^*\sim-\infty,\eta_2+\eta_2^*\sim 0),
\end{aligned}\tag{25}$$

where $\chi_i(x,y,t),\gamma_i(x,y,t)\ (i=1,2)$ are the real functions denoted as

$$\chi_i(x,y,t)=e^{-\sqrt{2}\Omega\,t}(\kappa_{iI}x+\iota_{iI}y)+\left(\kappa_{iI}^2-\kappa_{iR}^2+\iota_{iI}^2-\iota_{iR}^2\right)\frac{e^{-2\sqrt{2}\Omega\,t}}{2\sqrt{2}\Omega}+\frac{\sqrt{2}\Omega}{4}\left(x^2+y^2\right),$$
$$\gamma_i(x,y,t)=e^{-\sqrt{2}\Omega\,t}(\kappa_{iR}x+\iota_{iR}y)+\left(2\kappa_{iR}\kappa_{iI}+2\iota_{iR}\iota_{iI}\right)\frac{e^{-2\sqrt{2}\Omega\,t}}{2\sqrt{2}\Omega}+\eta_i^0. \tag{26}$$

Observing the asymptotic form of ϕ_{+1}^{1-} and ϕ_{+1}^{1+}, we calculate that the amplitudes, velocities, and structures of the solitons remain invariant during the interaction except for the initial phase. Therefore, the interaction of the two-solitons is elastic.

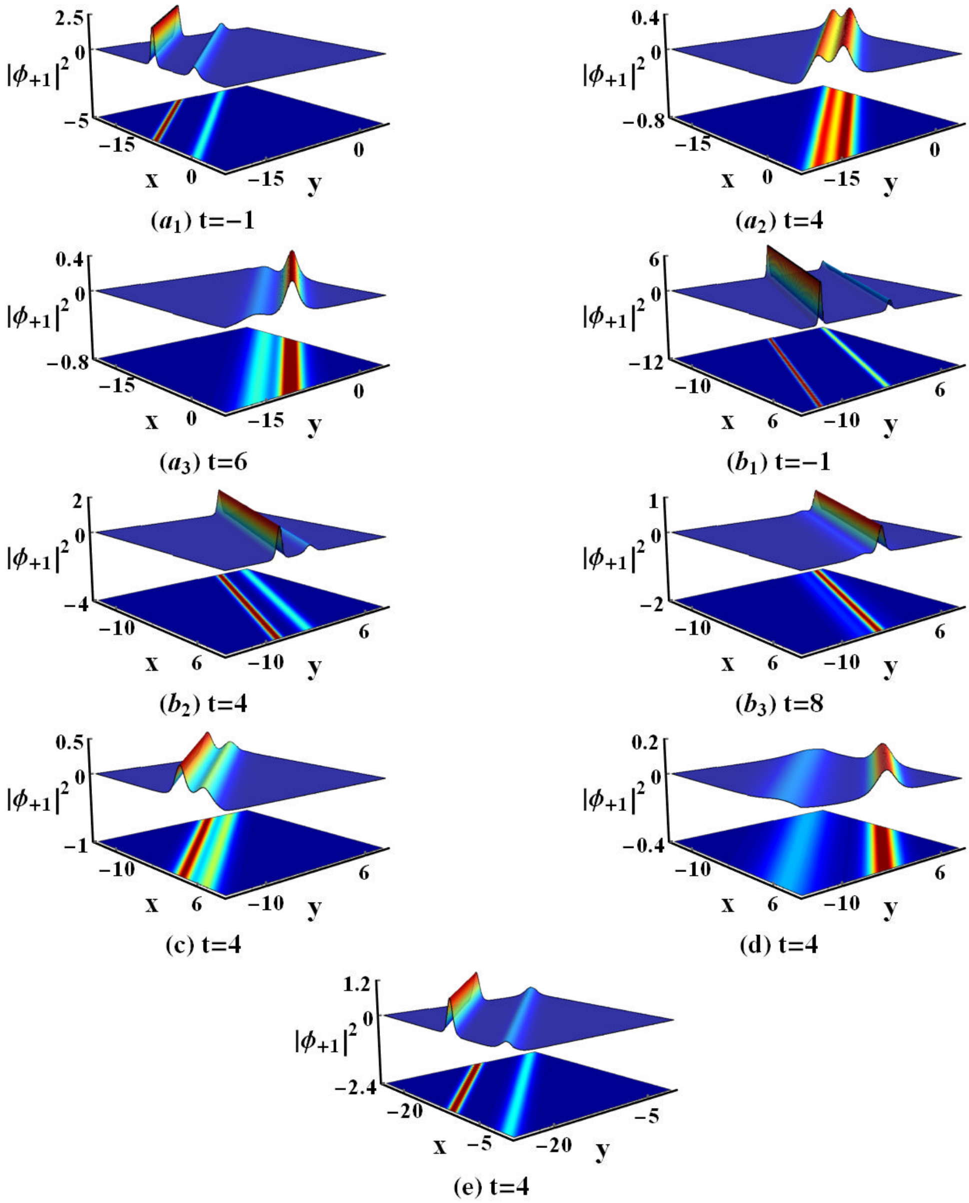

Fig. 3. The spatial-temporal evolution of the bright two-soliton via Eq. (10). The parameters are $\eta_0^1=1,\ \eta_0^2=-2,\ \alpha_0=-\sqrt{2}+i,\ \alpha_{-1}=1+\sqrt{2}i,\ \kappa_1=1+i/2,\ \kappa_2=2+i,\ \sigma=1$; (a) $\beta_{-1}=2-i,\ \iota_1=1+2i,\ \Omega=1/10$; (b) $\beta_{-1}=2-i,\ \iota_1=2-i/2,\ \Omega=1/10$; (c) $\beta_{-1}=1+i,\ \iota_1=1+2i,\ \Omega=1/10$; (d) $\beta_{-1}=2-i,\ \iota_1=1+2i,\ \Omega=1/4$; (e) $\beta_{-1}=2-i,\ \iota_1=1+2i,\ \Omega=1/20$.

The interaction of the bright two-soliton solution in the $x-y$ plane is shown in Fig. 3. Fig. 3a illustrates the overtaking interaction between bright two-solitons, where the bright two-solitons with different velocities move in the same direction, the bright soliton with a larger amplitude moves faster than the one with a smaller amplitude and overtakes the one with smaller amplitude after the interaction occurs. Fig. 3b shows the reciprocal interaction between bright two-solitons; the two-solitons with different velocities and amplitudes propagate along opposite directions and then separate after interaction at a certain time. Comparing from the three images separately, we can observe the amplitude of the two-solitons decreases with time t. Moreover, the interaction of the two-solitons does not affect the evolutionary trend of the soliton amplitude and velocity. Therefore, the interaction of the two-solitons is elastic; this property is consistent with the asymptotic analysis of the bright two-soliton Eq. (25). When fixed at the same t, the effects of the other parameters on the structure of the two-soliton are consistent with that of the one-soliton. Compared to Fig. 3a$_2$, Fig. 3c varies the parameter β_2, which influences the soliton velocity, shape, and direction of propagation. If the intensity of the harmonic potential parameter Ω is changed, the amplitude and velocity of solitons will undergo significant changes during propagation, as shown in Fig. 3d and Fig. 3e. The interaction time between two-solitons has changed; that is, it advances when the strength of Ω increases and delays when the strength of Ω decreases.

Next, we will discuss the dynamics of the interactions between the dark two-solitons by using the asymptotic analysis method to investigate the solutions of Eq. (17).

After expressing the equations between η_1 and η_2 according to Eq. (16), we can assume $(\iota_1^2+\kappa_1^2)\cot(\theta_1)\kappa_2<(\iota_2^2+\kappa_2^2)\cot(\theta_2)\kappa_1, \iota_1\kappa_2<\iota_2\kappa_1$, from the above relational equations, we summarize the asymptotic patterns, thus the mode-squared expressions for the dark two-soliton before and after the interaction $\left|\varphi_{+j}^{1-}\right|^2, \left|\varphi_{\pm j}^{1+}\right|^2$ $(j=1,2)$ are denoted respectively as

$$\begin{aligned}
&\left|\varphi_{+1}^{1-}\right|^2=M\left[1-\sin^2(\theta_1)\operatorname{sech}^2(\frac{\xi_1}{2})\right],\ (\xi_1\sim 0,\xi_2\sim-\infty),\\
&\left|\varphi_{+1}^{1+}\right|^2=M\left[1-\sin^2(\theta_1)\operatorname{sech}^2(\frac{\xi_1+\ln d_1}{2})\right],\ (\xi_1\sim 0,\xi_2\sim+\infty),\\
&\left|\varphi_{+2}^{1-}\right|^2=M\left[1-\sin^2(\theta_2)\operatorname{sech}^2(\frac{\xi_2+\ln d_1}{2})\right],\ (\xi_1\sim+\infty,\xi_2\sim 0),\\
&\left|\varphi_{+2}^{1+}\right|^2=M\left[1-\sin^2(\theta_2)\operatorname{sech}^2(\frac{\xi_2}{2})\right],\ (\xi_1\sim-\infty,\xi_2\sim 0).
\end{aligned} \tag{27}$$

where $M(t), \xi_i(x,y,t)$ $(i=1,2)$ are the real functions denoted as

$$\begin{aligned}
&M=e^{-2\sqrt{2\Omega t}}\left|p_1\right|^2,\\
&\xi_i=\kappa_i e^{-\sqrt{2}\Omega t}x+\iota_i e^{-\sqrt{2}\Omega t}y\\
&\quad-\left(\iota_i^2+\kappa_i^2\right)\cot(\theta)\frac{e^{-2\sqrt{2}\Omega t}}{2\sqrt{2}\Omega t}+\xi_i^0.
\end{aligned} \tag{28}$$

Since except for phase, the amplitude, width, and velocity of the dark two-soliton remain constant before and after the interaction, the dark two-soliton exhibits elastic interaction during propagation.

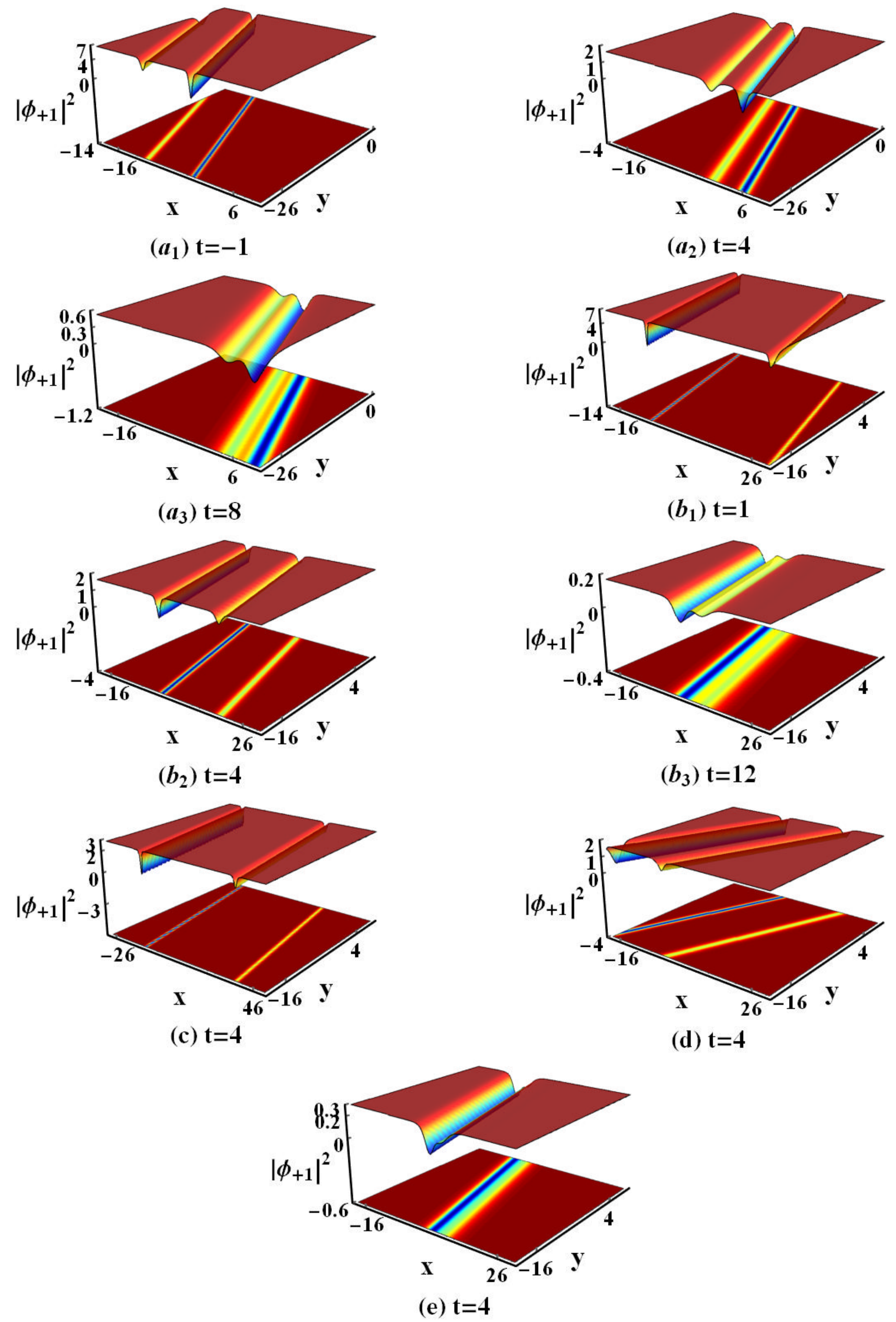

Fig. 4. The spatial-temporal evolution of the dark two-soliton via Eq. (17). The parameters are $\eta_0^1 = 1,\ \eta_0^2 = 1,\ \sigma = -1,\ p_1 = 2 + i,\ p_0 = 1 + i$; (a) $\Omega = 1/10,\ \iota_1 = 2,\ \theta_1 = 2\pi/3,\ \theta_2 = 4\pi/5$; (b) $\Omega = 1/10,\ \iota_1 = 2,\ \theta_1 = 2\pi/3,\ \theta_2 = \pi/5$; (c) $\theta_1 = 2\pi/3,\ \theta_2 = \pi/5,\ \Omega = 1/20,\ \iota_1 = 2$; (d) $\theta_1 = 2\pi/3,\ \theta_2 = \pi/5,\ \Omega = 1/20,\ \iota_1 = -3$; (e) $\theta_1 = 2\pi/3,\quad \theta_2 = \pi/5,\ \Omega = 1/4,\ \iota_1 = 2.$

Fig. 4 illustrates the dark two-soliton solution in terms of the coordinates x and y to discuss the interaction properties of the dark solitons. Fig. 4a depicts the overtaking interactions between the two dark solitons, namely, the dark two-soliton propagates in the same direction with different velocities. In Fig. 4b, dark two-soliton propagate along the opposite direction, approaching and interacting with each other. After the interaction, the amplitude and velocity changes of the two-solitons remain unchanged. Therefore, the dark two-soliton interaction is elastic, and this property is consistent with the asymptotic analysis of the dark two-soliton Eq. (27). At $t = 4$, the effect of different parameters on the soliton interaction is analyzed. In Fig. 4d, as the parameter ι_1 is varied, the propagation direction of the two-soliton changes, and the amplitude remains unchanged compared with Fig. 4b$_2$. In Fig. 4c, decreasing the strength of the harmonic potential parameter Ω, the background plane of the dark soliton is elevated while the soliton amplitude increases and two-soliton velocity decreases. In Fig. 4d, increasing the strength of harmonic potential Ω, the background plane of the dark soliton is lowered while the amplitude of two-solitons decreases; as the two-solitons are interact at this moment, the velocity increases.

5. Conclusion

In this paper, a (2+1)-dimensional three coupled GP system in spinor-1 BEC has been investigated by the Hirota method. Via constructing the bilinear forms of Eq. (3), bright one-solitons and bright two-solitons have been obtained when the system exhibits attractive interactions In contrast dark one-solitons and dark two-solitons have been obtained when the interactions is repulsive. We find that the amplitude of bright/dark solitons and the background plane of dark solitons decreases with the increase of harmonic potential strength, and vice versa. In addition, the elastic collision properties between solitons were discussed. These results may be helpful in understanding the dynamical behavior of localized waves in a (2+1)-dimensional spin-1 BECs. Lastly, we hope that the exact form of the soliton structures obtained here may be profitably exploited in designing the optimal BEC experiments.

Appendix

The parameters in Eq. (6) are listed as follows:

$$\omega_i(t) = -\frac{\mathrm{i}e^{-2\sqrt{2}\Omega\, t}(\iota_i^2+\kappa_i^2)}{2\sqrt{2}\Omega}, \beta_{+1} = \frac{\beta_0^2}{\beta_{-1}}, \alpha_{+1} = \frac{\alpha_0^2}{\alpha_{-1}}, \beta_0 = \frac{\alpha_0\beta_{-1}}{\alpha_{-1}},$$

$$\iota_2 = \frac{\iota_1^*(-\kappa_1+\kappa_2)+\iota_1(\kappa_1^*+\kappa_2)}{\kappa_1^*+\kappa_1}, n_5 = \frac{|L_1|^2(|\alpha_0|^2+|\alpha_{-1}|^2)\sigma}{|\alpha_0|^4 n_1\left[(\iota_2+\iota_2^*)^2+(\kappa_2+\kappa_2^*)^2\right]},$$

$$n_1 = \frac{(|\alpha_0|^2+|\alpha_{-1}|^2)\sigma}{|\alpha_{-1}|^4\left[(\iota_1+\iota_1^*)^2+(\kappa_1+\kappa_1^*)^2\right]}, n_3 = \frac{(|\alpha_0|^2+|\alpha_{-1}|^2)\beta_{-1}\sigma}{|\alpha_{-1}|^2\alpha_{-1}\left[(\iota_1+\iota_2^*)^2+(\kappa_1+\kappa_2^*)^2\right]},$$

$$n_2 = \frac{(|\alpha_0|^2+|\alpha_{-1}|^2)\sigma}{|\alpha_{-1}|^2\left[(\iota_2+\iota_2^*)^2+(\kappa_2+\kappa_2^*)^2\right]}, n_4 = \frac{(|\alpha_0|^2+|\alpha_{-1}|^2)\sigma}{|\alpha_{-1}|^2\alpha_{-1}^*\left[(\iota_2+\iota_1^*)^2+(\kappa_2+\kappa_1^*)^2\right]},$$

$$S_{+1} = \frac{n_2 n_3\alpha_0^2\alpha_{-1}^*\left[(\iota_1-\iota_2)^2+(\kappa_1-\kappa_2)^2\right]}{(|\alpha_0|^2+|\alpha_{-1}|^2)\sigma}, S_{-1} = \frac{S_{+1}\alpha_{-1}}{\alpha_0}, S_0 = \frac{S_{+1}\alpha_{-1}^2}{\alpha_0^2},$$

$$L_{+1}=\frac{n_1 n_4 \alpha_0^2 \alpha_{-1}^{*2}\left[\left(\iota_1-\iota_2\right)^2+\left(\kappa_1-\kappa_2\right)^2\right]}{(\left|\alpha_0\right|^2+\left|\alpha_{-1}\right|^2)\beta_{-1}^{*}\sigma}, L_{-1}=\frac{L_{+1}\alpha_{-1}}{\alpha_0}, L_0=\frac{L_{+1}\alpha_{-1}^2}{\alpha_0^2}.$$

The parameters in Eq. (10) are listed as follows:

$$\rho(t)=\frac{e^{-2\sqrt{2}\Omega\, t}\lambda}{2\sqrt{2}\Omega}, \lambda=-2\sigma(2\left|p_0\right|^2+\left|p_{+1}\right|^2+\left|p_{-1}\right|^2), p_{-1}=\frac{p_0^2}{p_{+1}}, \iota_2=\pm\iota_1\left|\frac{\sin(\theta_2)}{\sin(\theta_1)}\right|,$$

$$\omega_i(t)=-\frac{e^{-2\sqrt{2}\Omega\, t}(\iota_j^2+\kappa_j^2)\cot(\theta_i)}{2\sqrt{2}\Omega}, \kappa_i=\pm\sqrt{-\iota_j^2-\frac{4\sigma(\left|p_0\right|^2+\left|p_{+1}\right|^2)^2\sin^2(\theta_i)}{\left|p_{+1}\right|^2}},$$

$$d_j=A=-\frac{\left|p_{+1}\right|^2\left[(\iota_1-\iota_2)^2+(\kappa_1-\kappa_2)^2\right]-2\sigma(\left|p_0\right|^2+\left|p_{+1}\right|^2)^2(1-\cos[2(\theta_1-\theta_2)])}{\left|p_{+1}\right|^2\left[(\iota_1+\iota_2)^2+(\kappa_1+\kappa_2)^2\right]+2\sigma(\left|p_0\right|^2+\left|p_{+1}\right|^2)^2(1-\cos[2(\theta_1+\theta_2)])}.$$

Acknowledge. This work was supported by the Hubei Provincial Natural Science Foundation under Grant No. 2023AFB873.

Conflict of interest. The authors have declared that no conflict of interest exists.

References

1. Zhou, Q. (2022). Influence of parameters of optical fibers on optical soliton interactions. *Chinese Physics Letters*, *39*(1), 010501.
2. Zhou, Q., Zhong, Y., Triki, H., Sun, Y., Xu, S., Liu, W., & Biswas, A. (2022). Chirped bright and kink solitons in nonlinear optical fibers with weak nonlocality and cubic-quantic-septic nonlinearity. *Chinese Physics Letters*, *39*(4), 044202.
3. Soltani, M., Triki, H., Azzouzi, F., Sun, Y., Biswas, A., Yıldırım, Y., Alshehri, H. M. & Zhou, Q. (2023). Pure–quartic optical solitons and modulational instability analysis with cubic–quintic nonlinearity. *Chaos, Solitons & Fractals*, *169*, 113212.
4. Gao, P., Wu, Z., Yang, Z. Y., & Yang, W. L. (2021). Reverse Rotation of Ring-Shaped Perturbation on Homogeneous Bose–Einstein Condensates. *Chinese Physics Letters*, *38*(9), 090302.
5. He, J. T., Fang, P. P., & Lin, J. (2022). Multi-Type Solitons in Spin-Orbit Coupled Spin-1 Bose–Einstein Condensates. *Chinese Physics Letters*, *39*(2), 020301.
6. Cornell, E. A., & Wieman, C. E. (2002). Nobel Lecture: Bose-Einstein condensation in a dilute gas, the first 70 years and some recent experiments. *Reviews of Modern Physics*, *74*(3), 875.
7. Bloch, I., Dalibard, J., & Zwerger, W. (2008). Many-body physics with ultracold gases. *Reviews of Modern Physics*, *80*(3), 885.
8. Sekh, G. A., Pepe, F. V., Facchi, P., Pascazio, S., & Salerno, M. (2015). Split and overlapped binary solitons in optical lattices. *Physical Review A*, *92*(1), 013639.
9. Zhao, Y., Lei, Y. B., Xu, Y. X., Xu, S. L., Triki, H., Biswas, A., & Zhou, Q. (2022). Vector spatiotemporal solitons and their memory features in cold Rydberg gases. *Chinese Physics Letters*, *39*(3), 034202.
10. Ieda, J. I., Miyakawa, T., & Wadati, M. (2004). Exact analysis of soliton dynamics in spinor Bose-Einstein condensates. *Physical Review Letters*, *93*(19), 194102.
11. Pedri, P., & Santos, L. (2005). Two-dimensional bright solitons in dipolar Bose-Einstein condensates. *Physical Review Letters*, *95*(20), 200404.
12. Ding, C., Zhou, Q., Xu, S., Triki, H., Mirzazadeh, M., & Liu, W. (2023). Nonautonomous breather and rogue wave in spinor Bose–Einstein condensates with space-time modulated potentials. *Chinese Physics Letters*, *40*(4), 040501.
13. Feder, D. L., Pindzola, M. S., Collins, L. A., Schneider, B. I., & Clark, C. W. (2000). Dark-soliton states of Bose-Einstein condensates in anisotropic traps. *Physical Review A*, *62*(5), 053606.
14. Khaykovich, L., Schreck, F., Ferrari, G., Bourdel, T., Cubizolles, J., Carr, L. D., Castin, Y. & Salomon, C. (2002). Formation of a matter-wave bright soliton. *Science*, *296*(5571), 1290-1293.
15. Denschlag, J., Simsarian, J. E., Feder, D. L., Clark, C. W., Collins, L. A., Cubizolles, J., Deng, L., & Phillips, W. D. (2000). Generating solitons by phase engineering of a Bose-Einstein condensate. *Science*, *287*(5450), 97-101.
16. Frantzeskakis, D. J. (2010). Dark solitons in atomic Bose–Einstein condensates: from theory to experiments. *Journal of Physics A: Mathematical and Theoretical*, *43*(21), 213001.

17. Chomaz, L., Baier, S., Petter, D., Mark, M. J., Wächtler, F., Santos, L., & Ferlaino, F. (2016). Quantum-fluctuation-driven crossover from a dilute Bose-Einstein condensate to a macrodroplet in a dipolar quantum fluid. *Physical Review X*, *6*(4), 041039.
18. Chin, C., Grimm, R., Julienne, P., & Tiesinga, E. (2010). Feshbach resonances in ultracold gases. *Reviews of Modern Physics*, *82*(2), 1225.
19. Wu, B., Liu, J., and Niu, Q. (2002). Controlled generation of dark solitons with phase imprinting *Physical Review Letters, 88*, 034101.
20. Fritsch, A. R., Lu, M., Reid, G. H., Piñeiro, A. M., & Spielman, I. B. (2020). Creating solitons with controllable and near-zero velocity in Bose-Einstein condensates. *Physical Review A*, *101*(5), 053629.
21. Rizvi, S. T., Seadawy, A. R., Farah, N., & Ahmad, S. (2022). Application of Hirota operators for controlling soliton interactions for Bose-Einstien condensate and quintic derivative nonlinear Schrödinger equation. *Chaos, Solitons & Fractals*, *159*, 112128.
22. Xu, Y., Zhang, Y., & Wu, B. (2013). Bright solitons in spin-orbit-coupled Bose-Einstein condensates. *Physical Review A*, *87*(1), 013614.
23. Wang, H., Zhou, Q., & Liu, W. (2022). Exact analysis and elastic interaction of multi-soliton for a two-dimensional Gross-Pitaevskii equation in the Bose-Einstein condensation. *Journal of Advanced Research*, *38*, 179-190.
24. Wu, X. Y., Tian, B., Qu, Q. X., Yuan, Y. Q., & Du, X. X. (2020). Rogue waves for a (2+ 1)-dimensional Gross–Pitaevskii equation with time-varying trapping potential in the Bose–Einstein condensate. *Computers & Mathematics with Applications*, *79*(4), 1023-1030.
25. Hu, X. H., Zhang, X. F., Zhao, D., Luo, H. G., & Liu, W. M. (2009). Dynamics and modulation of ring dark solitons in two-dimensional Bose-Einstein condensates with tunable interaction. *Physical Review A*, *79*(2), 023619.
26. Gautam, S., & Adhikari, S. K. (2018). Three-dimensional vortex-bright solitons in a spin-orbit-coupled spin-1 condensate. *Physical Review A*, *97*(1), 013629.
27. De Izarra, G., Cerqueira, N., & De Izarra, C. (2011). Quantitative shadowgraphy on a laminar argon plasma jet at atmospheric pressure. *Journal of Physics D: Applied Physics*, *44*(48), 485202.
28. Chiacchio, E. R., & Nunnenkamp, A. (2019). Dissipation-induced instabilities of a spinor Bose-Einstein condensate inside an optical cavity. *Physical Review Letters*, *122*(19), 193605.
29. Kawaguchi, Y., & Ueda, M. (2012). Spinor bose–einstein condensates. *Physics Reports*, *520*(5), 253-381.
30. Nistazakis, H. E., Frantzeskakis, D. J., Kevrekidis, P. G., Malomed, B. A., & Carretero-González, R. (2008). Bright-dark soliton complexes in spinor Bose-Einstein condensates. *Physical Review A*, *77*(3), 033612.
31. Tojo, S., Hayashi, T., Tanabe, T., Hirano, T., Kawaguchi, Y., Saito, H., & Ueda, M. (2009). Spin-dependent inelastic collisions in spin-2 Bose-Einstein condensates. *Physical Review A*, *80*(4), 042704.
32. Wang, D. S., Shi, Y. R., Feng, W. X., & Wen, L. (2017). Dynamical and energetic instabilities of F= 2 spinor Bose–Einstein condensates in an optical lattice. *Physica D: Nonlinear Phenomena*, *351*, 30-41.
33. Hao, R., Li, L., Li, Z., & Zhou, G. (2004). Exact multisoliton solutions of the higher-order nonlinear Schrödinger equation with variable coefficients. *Physical Review E*, *70*(6), 066603.
34. Uchiyama, M., Ieda, J. I., & Wadati, M. (2006). Dark solitons in F= 1 spinor Bose–Einstein condensate. *Journal of the Physical Society of Japan*, *75*(6), 064002.
35. Dąbrowska-Wüster, B. J., Ostrovskaya, E. A., Alexander, T. J., & Kivshar, Y. S. (2007). Multicomponent gap solitons in spinor Bose-Einstein condensates. *Physical Review A*, *75*(2), 023617.
36. Xiong, B., & Gong, J. (2010). Dynamical creation of complex vector solitons in spinor Bose-Einstein condensates. *Physical Review A*, *81*(3), 033618.
37. Qin, Z., & Mu, G. (2012). Matter rogue waves in an F= 1 spinor Bose-Einstein condensate. *Physical Review E*, *86*(3), 036601.
38. Ding, C. C., Zhou, Q., Xu, S. L., Sun, Y. Z., Liu, W. J., Mihalache, D., & Malomed, B. A. (2023). Controlled nonautonomous matter–wave solitons in spinor Bose–Einstein condensates with spatiotemporal modulation. *Chaos, Solitons & Fractals*, *169*, 113247.
39. Kanna, T., Vijayajayanthi, M., & Lakshmanan, M. (2010). Coherently coupled bright optical solitons and their collisions. *Journal of Physics A: Mathematical and Theoretical*, *43*(43), 434018.
40. Sun, Y., Hu, Z., Triki, H., Mirzazadeh, M., Liu, W., Biswas, A., & Zhou, Q. (2023). Analytical study of three-soliton interactions with different phases in nonlinear optics. *Nonlinear Dynamics*, *111*(19), 18391-18400.
41. Zhou, Q., Huang, Z., Sun, Y., Triki, H., Liu, W., & Biswas, A. (2023). Collision dynamics of three-solitons in an optical communication system with third-order dispersion and nonlinearity. *Nonlinear Dynamics*, *111*(6), 5757-5765.
42. Zhou, Q., Sun, Y., Triki, H., Zhong, Y., Zeng, Z., & Mirzazadeh, M. (2022). Study on propagation properties of one-soliton in a multimode fiber with higher-order effects. *Results in Physics*, *41*, 105898.

43. Bersano, T. M., Gokhroo, V., Khamehchi, M. A., D'Ambroise, J., Frantzeskakis, D. J., Engels, P., & Kevrekidis, P. G. (2018). Three-component soliton states in spinor F=1 Bose-Einstein condensates. *Physical Review Letters*, *120*(6), 063202.
44. Doktorov, E. V., Rothos, V. M., & Kivshar, Y. S. (2007). Full-time dynamics of modulational instability in spinor Bose-Einstein condensates. *Physical Review A*, *76*(1), 013626.
45. Dalfovo, F., Giorgini, S., Pitaevskii, L. P., & Stringari, S. (1999). Theory of Bose-Einstein condensation in trapped gases. *Reviews of Modern Physics*, *71*(3), 463.
46. Zhong, H., Tian, B., Jiang, Y., Li, M., Wang, P., & Liu, W. J. (2013). All-optical soliton switching for the asymmetric fiber couplers. *The European Physical Journal D*, *67*, 1-15.
47. Hirota, R. (1971). Exact Solution of the Korteweg—de Vries Equation for Multiple Collisions of Solitons. *Physical Review Letters, 27*, 1192–4.

Nan Li, Quan Chen, Houria Triki, Feiyan Liu, Yunzhou Sun, Siliu Xu, Qin Zhou. (2024). Bright and Dark Solitons in a (2+1)-Dimensional Spin-1 Bose-Einstein Condensates**.** *Ukrainian Journal of Physical Optics*, ***25*(5),** S1060 – S1074.
doi: 10.3116/16091833/Ukr.J.Phys.Opt.2024. S1060

Анотація. *У цій статті досліджується тризв'язане рівняння Гросса-Пітаєвського з гармонічним потенціалом у (2+1)-вимірному бозе-ейнштейнівському конденсаті зі спіном-1. За допомогою білінійного методу Хіроти отримано світлі та темні солітонні розв'язки системи з взаємодіями притягання та відштовхування, а також наведено амплітуди та швидкості цих солітонів. Крім того, проаналізовано вплив гармонічного потенціалу на динаміку солітонів і досліджується взаємодія між солітонами за допомогою асимптотичного аналізу. У результаті виявлено, що амплітуда і швидкість солітонів пов'язані з гармонічним потенціалом, а взаємодія між двома солітонами є пружною.*

Ключові слова: *солітон, білінійний метод Хірота, асимптотичний аналіз, конденсат Бозе-Ейнштейна*